Characterizing Bathocuproine Self-association and Subsequent Binding to Alzheimer's Disease Amyloid β-Peptide by NMR

SHENGGEN YAO,[a]* ROBERT A CHERNY,[b] ASHLEY I. BUSH,[b,c] COLIN L. MASTERS,[b] and KEVIN J. BARNHAM[b]*

[a] The Walter and Eliza Hall Institute of Medical Research, and The Cooperative Research Center for Cellular Growth Factors, 1G Royal Parade, Parkville, VIC 3050, Australia
[b] Department of Pathology, The University of Melbourne, and The Mental Health Research Institute of Victoria, Parkville VIC 3010, Australia
[c] Laboratory for Oxidation Biology, Genetics and Aging Unit and Department of Psychiatry, Harvard Medical School, Massachusetts General Hospital East, Charlestown, MA 02129 USA

Abstract: Aggregated amyloid β-peptide (Aβ) is the primary constituent of the extracellular plaques and perivascular amyloid deposits associated with Alzheimer's disease (AD). Deposition of the cerebral amyloid plaques is thought to be central to the disease progression. One such molecule that has previously been shown to 'dissolve' deposited amyloid in post-mortem brain tissue is bathocuproine (BC). In this paper ^{1}H NMR chemical shift analysis and pulsed field gradient NMR diffusion measurements were used to study BC self-association and subsequent binding to Aβ. The results show that BC undergoes self-association as its concentration increases. The association constant of BC dimerization, K_a, was estimated to be 0.64 mM^{-1} at 25 °C from ^{1}H chemical shift analysis. It was also found that dimerization of BC appeared to be essential for its binding to Aβ. From the self-association constant of BC, K_a, the fraction of dimeric BC in the complex was obtained and the dissociation constant, K_d, of BC bound to Aβ40 peptide was then determined to be ~1 mM. Copyright © 2003 European Peptide Society and John Wiley & Sons, Ltd.

Keywords: Alzheimer's disease; amyloid β-peptide; bathocuproine; ligand binding; NMR; self-association; translational diffusion

INTRODUCTION

Alzheimer's disease (AD) is characterized by extracellular deposits in the brain. The major constituent

* Correspondence to: Kevin J. Barnham, Department of Pathology, The University of Melbourne, Parkville, VIC 3010, Australia; e-mail: kbarnham@unimelb.edu.au

of these deposits is amyloid β-peptide (Aβ), a normally soluble 4.3 kDa peptide found in all biological fluids [1]. It is believed that Aβ interacts with transition metals leading to peptide aggregation and with redox active metals to generate reactive oxygen species [2,3]. This is significant as there is mounting evidence that oxidative stress causing cellular damage is central to the neurodegeneration of AD [4,5]. Increases in oxidation of proteins as well as nuclear and mitochondrial DNA in AD brains [6–8], and the ability of Aβ to enhance the generation of reactive oxygen species (ROS) in cells of neural origin as well as in cell free media [9–11] have been reported. Elevated levels of Cu (400 μM), Zn (1 mM) and Fe (1 mM) have been found in amyloid deposits in AD-affected

brains [12,13] and it has been observed that senile plaques and neurofibrillary tangles isolated from AD brains were capable of generating ROS mediated by bound copper and iron [14].

There is growing evidence that metals such as copper, zinc and iron coordinate to Aβ and play a deleterious role in Alzheimer's disease, through inducing aggregation of the peptide and instigating redox chemical reactions to produce H_2O_2 and ROS via Fenton chemistry. This suggests a potential therapeutic strategy, i.e. to interfere with the Aβ/metal interaction. The use of compounds that will compete with Aβ for the metal ions (i.e. metal-chelating compounds) have already shown some very promising results both *in vitro* and *in vivo* [15–17]. It has been shown that the solubilization of Aβ from postmortem brain tissue of AD patients was increased in the presence of metal chelators including clioquinol, *N,N,N,N*-tetrakis(2-pyridyl-methyl) ethylene diamine and bathocuproine [13–15]. Our studies on the interactions of compounds that chelate metal ions from Aβ have led to the surprising observation that bathocuproine disulfonic acid (BC) (Figure 1), a Cu(I) specific chelator and the structurally related bathophenanthroline disulfonic acid (BP) have an intrinsic affinity for Aβ peptides. The NMR studies presented here aim to provide further insight into the interactions between BC and Aβ.

The process of molecular association or recognition induces local and global changes to the molecules involved, which alter their physical and chemical behaviour in solution. Changes in chemical shifts, relaxation rates and molecular translation self-diffusion coefficients as can be readily measured by NMR have been frequently used to monitor the processes of association and recognition with the equilibrium constants to be determined from titration experiments [18,19]. This paper reports results from studies of BC self-association and binding to the amyloid β-peptide (Aβ), by monitoring changes of NMR chemical shifts and translational diffusion coefficients.

MATERIALS AND METHODS

Sample Preparation

Bathocuproine-3,4-disulfonic acid and Congo red were purchased from Sigma. Phthalocyanine tetrasulfonate was purchased from Porphyrin Products (Logan Utah). A stock BC sample was prepared by dissolving 25 mg BC in 1 ml phosphate (50 mM) buffered saline (100 mM) at pH 6.9. The sample was then diluted using the same buffer to the desired concentration. Aqueous Aβ peptide solutions (0.23 mM) for NMR studies were prepared as previously described [20].

NMR Spectroscopy

NMR spectra were acquired at 25 °C on Bruker DRX600 and AMX500 spectrometers using 5 mm triple resonance probes equipped with either triple gradients or a single gradient (Z). Calibrations of the B_0 field gradient strengths were carried out as previously described [21]. One-dimensional spectra were recorded using a standard watergate pulse sequence [22]. ^{1}H chemical shift was referenced to DSS (2,2-dimethyl-2-silapentane-5-sulfonate) at 0 ppm indirectly via the H_2O signal of 4.766 ppm at 25 °C [23]. A conventional LEDSTE sequence with crusher gradients during both longitudinal storage periods was used for diffusion measurements [24,25]. Water suppression was achieved by incorporating a watergate segment into the RF pulse sequence before the signal acquisition [22]. For diffusion measurements, a series of 12 diffusion weighted spectra were recorded in a 2D manner for each measurement with a recycle time of 2 s and 16 to 256 scans were used for each spectrum depending on the concentration of the sample. All spectra were processed using XWINNMR 2.6 (Bruker). Translational diffusion coefficients, *D*, were obtained using the program *Simfit* (Bruker) by fitting intensities of the BC methyl resonance to Equation (1)
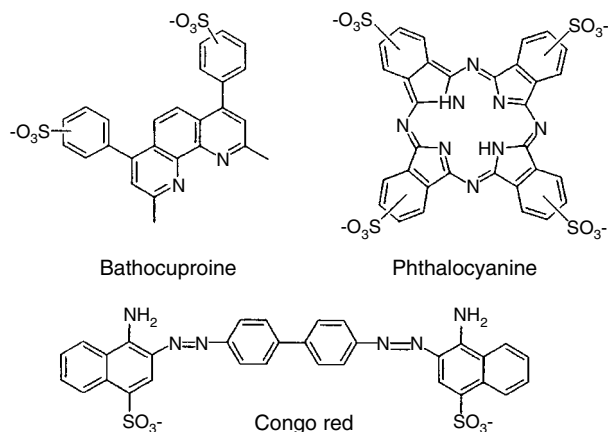
Figure 1   Chemical structures of molecules that bind to Aβ.

$$I = I_0 \exp(-\gamma^2 g^2 \delta^2 (\Delta - \delta/3)D) \qquad (1)$$

where γ is the gyromagnetic ratio of the observed nucleus and g, δ and Δ are the amplitude, duration and separation of the single pair gradient pulses, respectively [26]. For D_{free} and D_{obs} (diffusion coefficient of BC in the absence and presence of Aβ peptide) a total of six peaks from BC across the spectrum were used for the calculation at each given concentration and the averaged values are reported. For D_{bound} (diffusion coefficient of BC bound to Aβ peptide), five peaks from the upper field region of Aβ peptide were used for the calculation and the averaged values are presented.

Determination of the Equilibrium Constants

For molecules undergoing self-association and modelled by a monomer–dimer equilibrium, its association constant, K_a, can be obtained by fitting chemical shifts (δ) or diffusion coefficients (D) measured at a number of concentrations according to the following relationships

$$P_{\text{obs}} = \alpha_1 P_m + (1 - \alpha_1)P_d \tag{2}$$

$$K_a = (1 - \alpha_1)C_t/2(\alpha_1 C_t)^2 \tag{3}$$

where P_{obs} represents either the experimentally measured chemical shift (δ_{obs}) or diffusion coefficient (D_{obs}) of the molecule at a given concentration, P_m is the corresponding parameter for the molecule in its monomeric form, (δ_m or D_m), while P_d represents δ_d or D_d of the dimer. α_1 is the mole fraction of monomer and C_t is the total molar concentration of the molecule [18].

In most ligand and receptor systems where free and bound ligands are under fast exchange, the observed ligand diffusion coefficient will be the mole fraction weighted average of the diffusion coefficients of free and bound ligands [19]. If β_1 is the fraction of ligand bound to the receptor

$$D_{\text{obs}} = (1 - \beta_1)\, D_{\text{free}} + \beta_1\, D_{\text{bound}} \tag{4}$$

where D_{free} and D_{obs} are diffusion coefficients of the ligand in the absence and presence of the receptor molecule and D_{bound} is the diffusion coefficient of the ligand bound to the receptor molecule. Since Equation (4) has exactly the same form as Equation (2), the dissociation constant, K_d, can then be obtained by measuring the D_{obs} values as a function of ligand concentration and then fitting the data to Equation (4) together with

$$K_d = (L_{\text{tot}}/\beta_1)[\beta_1{}^2 - \beta_1(1 + P_{\text{tot}}/L_{\text{tot}}) + P_{\text{tot}}/L_{\text{tot}}] \tag{5}$$

where L_{tot} and P_{tot} are concentrations of total ligand and receptor in the complex system. Equations (4) and (5) can also be used to estimate the ligand binding constants from other NMR parameters, e.g. chemical shifts (δ) and relaxation rates (R_1 or R_2) [19]. In particular, if diffusion coefficients of the free ligand, receptor and ligand/receptor complex are measured, then the K_d value for the complex may be calculated directly at a single concentration of ligand and receptor from Equation (5). This may not be possible for NMR parameters such as chemical shift or relaxation rates since the values of these parameters of the bound form are usually not directly measurable.

RESULTS

Self-association of Bathocuproine

A stack plot of the ^{1}H NMR spectra of BC at a number of concentrations is depicted in Figure 2. As the concentration of BC increases, it shows a characteristic upfield shift of all resonances. No significant changes were observed in terms of chemical shifts and diffusion coefficients for measurements taken several days apart at a given BC concentration. Chemical shift changes of three selected resonances (Figure 2) and translational diffusion coefficients of BC as a function of molar concentrations of BC are shown in Figure 3. The continual shifting of its resonances and the consistent decline of its apparent translational diffusion coefficient with increasing concentration indicates that BC undergoes self-association. The
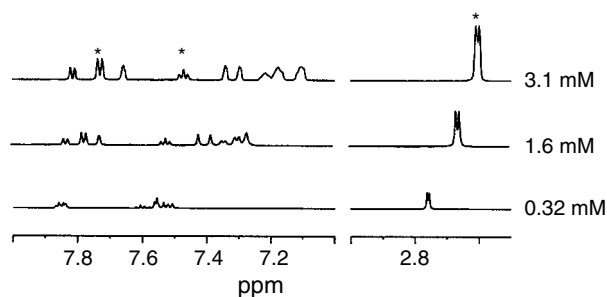
Figure 2   Stack plot of 600 MHz ^{1}H spectra of BC showing its dependence upon increasing BC concentration. The shift in the ^{1}H NMR peaks with increasing concentration is indicative of a system undergoing fast exchange on the NMR timescale. This rate of exchange is consistent with dissociation constants in the millimolar range. Peaks marked with * indicate those used to generate Figure 3a.
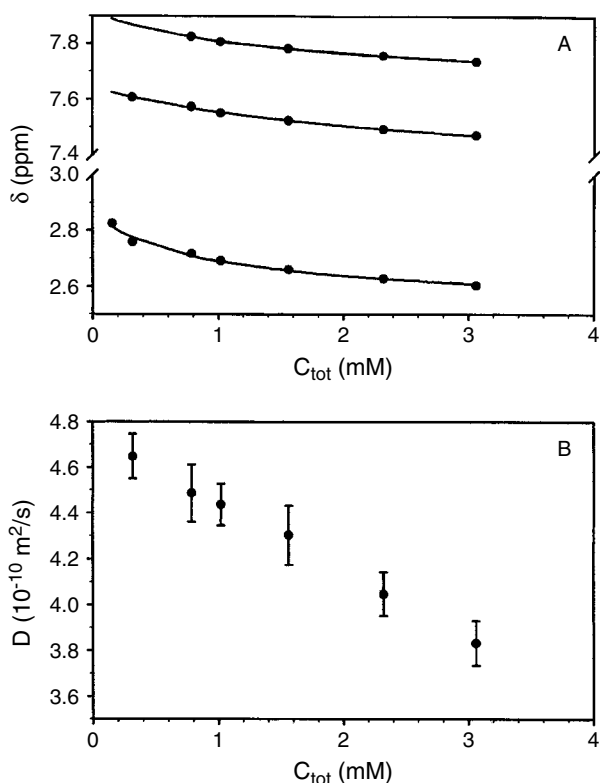
Figure 3 Plots of chemical shifts (A) and translational diffusion coefficients (B) of BC as a function of its molar concentration. Lines in (A) represent fits to a monomer–dimer equilibrium model, Equations (2) and (3).

chemical shift data as shown in Figure 3A were fitted to a monomer–dimer equilibrium (Equations (2) and (3)) and gave a resultant K_a value of (0.64 ± 0.36) mM^{-1}.

Estimation of K_d value of BC Bound to Aβ40 Peptide

As has been previously reported [16], when BC is titrated into an aqueous solution of Aβ40, changes occur in the NMR spectrum that are consistent with an equilibrium between BC bound to Aβ and free ligand undergoing fast exchange on the NMR timescale. Figure 4 shows the logarithm of the intensity of the methyl peak of BC (1.6 mM) versus the strength of diffusion encoding used to determine the diffusion coefficients of D_{free}, D_{obs} and D_{bound} (+Aβ40). The diffusion data of all three forms were fitted to Equation (1), a single exponential decay. Experimentally measured diffusion coefficients, D_{free}, D_{obs} and D_{bound} as a function of BC concentration are shown in Figure 5.
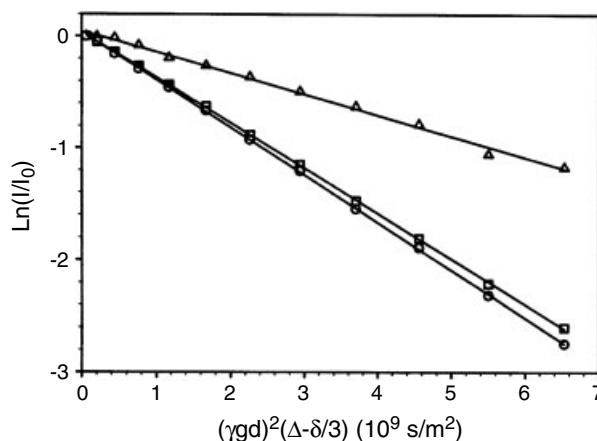

Figure 4 Logarithmic spectral intensities of BC (1.6 mM) in the absence (○) and presence (□) of 0.23 mM Aβ40 peptide together with spectral intensities of Aβ40 (△) versus the strength of diffusion encoding, $\gamma^2 g^2 \delta^2 (\Delta - \delta/3)$. Lines represent the results of non-linear regression to Equation (1) illustrating excellent fits of spectral intensities of all three forms of BC to a single exponential decay, which indicates the processes of BC self-association and binding to Aβ40 are within the fast exchange regime on the NMR time scale.
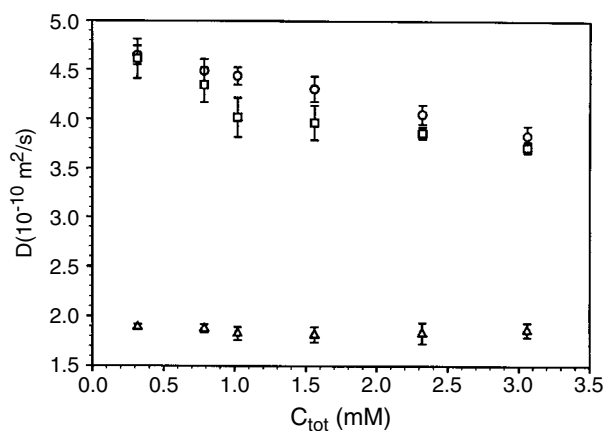

Figure 5 Experimentally measured diffusion coefficients of BC in the absence (D_{free}: ○) and presence (D_{obs}: □, D_{bound}: △) of 0.23 mM Aβ 40 as a function of BC molar concentration. As the concentration of BC increased, no significant changes were observed for the D_{bound}, whereas changes to D_{obs} compared with D_{free} were clearly evident indicating BC bound to Aβ.

For concentrations of BC below 0.32 mM corresponding to a fraction of dimer less than 20% (see Table 1), no perturbation of the Aβ40 ^{1}H NMR spectrum was observed. This suggests that significant binding of BC to Aβ does not occur until a

critical percentage of dimer of BC is formed. Using the self-association K_a values derived from chemical shift data shown in Figure 3A, fractions of dimer at each concentration were determined from Equations (2) and (3). The fractions of dimeric BC bound to Aβ40 were estimated from experimentally measured diffusion coefficients using Equation (4), where contributions from crowding and viscosity are assumed as being negligible at a given concentration of BC. From the fractions of dimer, K_d values of BC bound to Aβ40 peptide under the assumption of a 1:1 complex were then determined from Equation (5). The results are summarized in Table 1. The results suggest that significant binding does not occur until a fraction of dimer around 40% is reached.

Other Related Compounds

To determine if the increase in binding affinity between Aβ and BC when BC dimerizes was the result of an increased aromatic surface for the peptide to interact with, a solution of Cu(BC)$_2$, a very stable Cu(I) complex with two BC ligands arranged about the copper in a tetrahedral coordination sphere were prepared and the interactions of this molecule with Aβ were examined. An aqueous solution of Cu(BC)$_2$ was then added to an Aβ solution at a concentration (0.16 mM) in which BC itself was not significantly aggregated and has no measurable affinity for Aβ. Changes were observed

Table 1 Fractions of Dimeric Form of BC in Solution and K_d Values in Binding to Aβ40 Peptide

$C_{tot}(L_{tot}, \text{mM})^{a}$	Fraction of dimer $(1 - \alpha_1)$	$K_d(\text{mM})^{b}$
0.32	0.23	18.9
0.79	0.38	5.0
1.02	0.42	1.0
1.56	0.50	1.1
2.32	0.56	2.0
3.16	0.60	2.7

[a] Total molar concentration of BC in the absence or presence of Aβ40 peptide.
[b] Calculated using Equation (5) assuming BC binds to Aβ40 in a dimeric form with a total concentration of dimer given by $L'_{tot} = (1 - \beta_1)L_{tot}/2$. Also estimated from diffusion measurements, Cu(BC)$_2$ binds to Aβ40 with a K_d of 0.9 mM^{-1}.

in the NMR spectrum, which were consistent with Cu(BC)$_2$ binding to Aβ in a similar fashion to the dimeric BC which only forms at higher concentrations. It was determined via diffusion measurements that the binding affinity of Cu(BC)$_2$ to Aβ was 0.9 mM.

In the light of these results, two other sulfonated aromatic compounds were investigated for their possible interactions with Aβ, Congo red and phthalocyanine tetra sulfonate. Phthalocyanine (Figure 1) is a planar molecule with a high aromatic character. ^{1}H NMR spectra indicated that similar interactions occur between Aβ and phthalocyanine tetrasulfonate when the molecule was titrated into aqueous solutions of Aβ as was observed for the phenanthroline derivatives. The aromatic residues Y10, F4, F19 of Aβ are most effected by the presence of phthalocyanine, except that rather than the chemical shift of peaks shifting in fast exchange as was observed for the 1,10 phenanthroline derivatives, they were broadened beyond detection (Figure 6). This significant line broadening matches the characteristic of intermediate exchange on the NMR timescale and thus the rate of exchange is typically around micromolar affinity. Attempts to determine accurately the binding constants by NMR were, however, compromised by the signal broadening due to the intermediate exchange that lead to undetectable signals. Similar results were observed when Congo red was titrated into an aqueous solution of Aβ. While the initial spectrum of Congo red is quite broad due to self-association [27] changes in the NMR

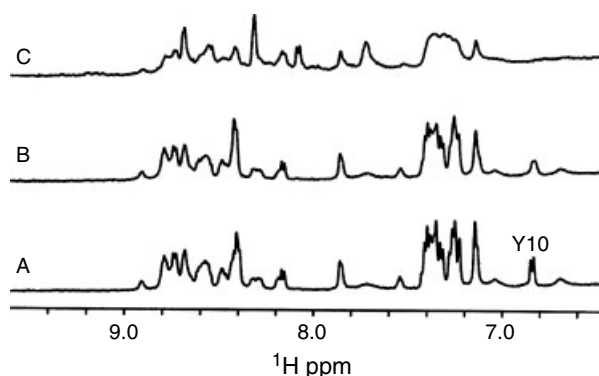**Figure 6** Stack plot of 600 MHz ^{1}H spectra of Aβ (A) with increasing concentration of phthalocyanine tetrasulfonate titrated into the aqueous solution (B, C). The broadening beyond detection of the Hε peaks of Y10 is indicative of a system undergoing intermediate exchange on the NMR timescale. This rate of exchange is consistent with dissociation constants in the micromolar range.

spectrum of Aβ are consistent with Congo red binding to the aromatic residues in the *N*-terminal half of Aβ. As with phthalocyanine, it was not possible to determine accurately the binding constants due to intermediate exchange phenomena broadening peaks beyond detection.

DISCUSSION

Molecular self-diffusion coefficients measured by NMR have recently been used to investigate the self-association behaviours of proteins and peptides in solution [21,25,28]. Self-association constants under the assumption of a monomer–dimer equilibrium have also been determined successfully from measured diffusion coefficients without making any corrections to account for changes in solution conditions as the protein concentration increases [29,30].

The estimation of ligand binding affinity via NMR diffusion measurements relies on an accurate determination of translational diffusion coefficients of the ligand in all three forms (D_{free}, D_{obs} and D_{bound}). Clearly, the method suits systems where free and bound ligands are in rapid exchange on the NMR time scale (i.e. relatively weak binding) and an excess of free ligand is present. For situations where free and bound ligands are under intermediate exchange, reliable measurements of D_{obs} may not be possible due to the excessive broadening of the NMR spectral line-width as observed for Aβ plus phthalocyanine tetrasulfonate and Congo red.

In the present study, experimentally measured chemical shifts and translational diffusion coefficients of BC up to a concentration of 3 mM as shown in Figure 3 provide clear evidence that BC undergoes self-association in solution as the concentration increases. The chemical shift data as shown in Figure 3a were consistent with a monomer–dimer equilibrium. The measured diffusion coefficients of BC show a reduction from $(4.7 \pm 0.1) \times 10^{-10}$ m^2/s at 0.32 mM to $(3.8 \pm 0.1) \times 10^{-10}$ m^2/s at 3.1 mM a decrease of 19% as would be expected upon dimerization (in a hard sphere model [31]). However, attempts to fit the data (Figure 3b) to a monomer–dimer equilibrium were not successful. This is not surprising since chemical shift changes of a given nuclear spin group mainly reflect changes of its local chemical environment, e.g. due to molecular stacking whereas a reduction in the translational diffusion coefficient may also result from changes other than molecular aggregation. A similar example has been reported recently by Price *et al.* [32],

in a study of lysozyme aggregation in solution. In that study, diffusion coefficients of lysozyme were measured up to a concentration of 6 mM in the presence of 0.5 M NaCl that clearly indicated self-association, but the diffusion data could not be fitted to a monomer–dimer equilibrium model unless the solution crowding effects were taken into account. Therefore, it is concluded that apart from the possible presence of small fractions of higher aggregate forms, contributions from changes of sources other than BC aggregation as a result of increasing concentration may be responsible for the failure of its measured diffusion coefficients to be fitted to a monomer–dimer equilibrium.

The nature of the BC self-association is, however, difficult to define but it is presumably due to aromatic stacking interactions. Perusal of examples of intermolecular aromatic/aromatic interactions depicted in the x-ray structures of a range of BC/BP molecules present in the Cambridge structural database (CSD) suggests there is no single favoured stacking arrangement. The stacking arrangements are varied, for example the crystal structure of BP has the aromatic ring attached at position four and seven stacked over the middle ring of the phenanthroline moiety of another BP molecule. Metal complexed structures of BC and BP have other stacking arrangements the most common being the stacking of the phenanthroline moieties on top of each other, although again these stacking interactions varied as there is no consistent angle between the stacked phenanthroline rings. Unfortunately there is no crystal structure of BC alone or sulfonated phenanthroline derivatives.

Analysis of the data presented in this study indicates that BC has no interactions with Aβ at concentrations where there is effectively only monomeric BC in solution, i.e. BC dimerization is critical to Aβ binding. The nature of the dimerization could not be determined although it is likely to involve some type of stacking of aromatic rings. Cu(BC)$_2$ has a tetrahedral coordination sphere about the metal ion and as such there is no possible aromatic stacking between the BC ligands coordinated to the copper. The relative orientation of BC in this molecule must be different from that in the BC dimer. As both molecules have an affinity for Aβ this suggests that this affinity is not the result of a single structural motif. In all probability the increased affinity of Cu(BC)$_2$ for Aβ reflects a larger aromatic surface area for Aβ to interact with. Indeed a large aromatic surface area would also explain the higher affinities of Congo red and

phthalocyanine for Aβ. It was previously shown that when BC was titrated into an aqueous solution of Aβ changes were observed in the ¹H NMR spectra consistent with BC binding to the aromatic residues F4, Y10 and F19 [16]. These results suggest that some aromatic–aromatic interaction (e.g. stacking) may be occurring between Aβ peptides and BC.

In conclusion, with the application of NMR chemical shift analysis and translational diffusion measurements both the self-association constant of BC and the binding constant of it bound to Aβ40 peptide have been determined. The results suggest that BC only has a measurable affinity for Aβ at concentrations where it oligomerizes, this does not occur until the molecule reaches millimolar concentrations. Therefore, potential therapeutic applications of BC and BP are limited. However, other aromatic compounds have shown much higher affinity for Aβ and as such there is the potential to design aromatic compounds that have sufficiently high affinity to Aβ to be useful for therapeutic/diagnostic applications in AD.

Acknowledgements

REFERENCES

1. Masters CL, Simms G, Weinman NA, Multhaup G, McDonald BL, Beyreuther K. Amyloid plaque core protein in Alzheimer disease and Down syndrome. *Proc. Natl Acad. Sci. USA* 1985; **82**: 4245–4249.

2. Huang X, Atwood CS, Moir RD, Hartshorn MA, Vonsattel JP, Tanzi RE, Bush AI. Zinc-induced Alzheimer's Aβ 1–40 aggregation is mediated by conformational factors. *J. Biol. Chem.* 1997; **272**: 26 464–26 470.

3. Atwood CS, Moir RD, Huang X, Scarpa RC, Bacarra NME, Romano DM, Hartshorn MA, Tanzi RE, Bush AI. Dramatic aggregation of Alzheimer Aβ by Cu(II) is induced by conditions representing physiological acidosis. *J. Biol. Chem.* 1998; **273**: 12 817–12 826.

4. Martins RN, Harper CG, Stokes GB, Masters CL. Increased cerebral glucose-6-phosphate-dehydrogenase activity in Alzheimer's disease may reflect oxidative stress. *J. Neurochem.* 1986; **46**: 1042–1045.

5. Multhaup G, Masters CL, Beyreuther K. Oxidative stress in Alzheimer's disease. Alzheimer's Rep. 2000; **1**: 147–154.

6. Gabbita SP, Lovell MA, Markesbery WR. Increased nuclear DNA oxidation in the brain in Alzheimer's disease. *J. Neurochem.* 1998; **71**: 2034–2040.

7. Markesbery WR. Oxidative stress hypothesis in Alzheimer's disease. *Free Radic. Biol. Med.* 1997; **23**: 134–147.

8. Cuajungco MP, Goldstein LE, Nunomura A, Smith MA, Lim JT, Atwood CS, Huang X, Farrag YW, Perry G, Bush AI. Evidence that the β-amyloid plaques of Alzheimer's disease represent the redox-silencing and entombment of Aβ by zinc. *J. Biol. Chem.* 2000; **275**: 19 439–19 442.

9. Behl C, Davis JB, Lesley R, Schubert D. Hydrogen-peroxide mediates amyloid-β protein toxicity. *Cell* 1994; **77**: 817–827.

10. Huang X, Cuajungco MP, Atwood CS, Hartshorn MA, Tyndall JD, Hanson GR, Stokes KC, Leopold M, Multhaup G, Goldstein LE, Scarpa RC, Saunders AJ, Lim J, Moir RD, Glabe C, Bowden EF, Masters CL, Fairlie DP, Tanzi RE, Bush AI. Cu(II) potentiation of Alzheimer Aβ neurotoxicity — correlation with cell-free hydrogen peroxide production and metal reduction. *J. Biol. Chem.* 1999; **274**: 37 111–37 116.

11. Huang X, Atwood CS, Hartshorn MA, Multhaup G, Goldstein LE, Scarpa RC, Cuajungco MP, Gray DN, Lim J, Moir RD, Tanzi RE, Bush AI. The Aβ peptide of Alzheimer's disease directly produces hydrogen peroxide through metal ion reduction. *Biochemistry* 1999; **38**: 7609–7616.

12. Lovell MA, Robertson JD, Teesdale WJ, Campbell JL, Markesbery WR. Copper, iron and zinc in Alzheimer's disease senile plaques. *J. Neurol. Sci.* 1998; **158**: 47–52.

13. Smith MA, Harris PLR, Sayre LM, Perry G. Iron accumulation in Alzheimer disease is a source of redox-generated free radicals. *Proc. Natl Acad. Sci. USA* 1997; **94**: 9866–9868.

14. Sayre LM, Perry G, Harris PL, Liu Y, Schubert KA, Smith MA. *In situ* oxidative catalysis by neurofibrillary tangles and senile plaques in Alzheimer's disease: A central role for bound transition metals. *J. Neurochem.* 2000; **74**: 270–279.

15. Cherny RA, Legg JT, McLean CA, Fairlie DP, Huang X, Atwood CS, Beyreuther K, Tanzi RE, Masters CL, Bush AI. Aqueous dissolution of Alzheimer's disease Aβ amyloid deposits by biometal depletion. *J. Biol. Chem.* 1999; **274**: 23 223–23 228.

16. Cherny RA, Barnham KJ, Lynch T, Volitakis I, Li QX, McLean CA, Multhaup G, Beyreuther K, Tanzi RE, Masters CL, Bush AI. Chelation and intercalation: Complementary properties in a compound for the treatment of Alzheimer's disease. *J. Struct. Biol.* 2000; **130**: 209–216.

17. Cherny RA, Atwood CS, Xilinas ME, Gray DN, Jones WD, McLean CA, Barnham KJ,

Volitakis I, Fraser FW, Kim Y, Huang X, Goldstein LE, Moir RD, Lim JT, Beyreuther K, Zheng H, Tanzi RE, Masters CL, Bush AI. Treatment with a copper-zinc chelator markedly and rapidly inhibits β-amyloid accumulation in Alzheimer's disease transgenic mice. *Neuron* 2001; **30**: 665–676.

18. Martin RB. Comparisons of indefinite self-association models. *Chem. Rev.* 1996; **96**: 3043–3064.

19. Fielding L. Determination of association constants (K_a) from solution NMR data. *Tetrahedron* 2000; **56**: 6151–6170.

20. Curtain CC, Ali F, Volitakis I, Cherny RA, Norton RS, Beyreuther K, Barrow CJ, Masters CL, Bush AI, Barnham KJ. Alzheimer's disease amyloid-β binds copper and zinc to generate an allosterically ordered membrane-penetrating structure containing superoxide dismutase-like subunits. *J. Biol. Chem.* 2001; **276**: 20 466–20 473.

21. Yao S, Howlett GJ, Norton RS. Peptide self-association in aqueous trifluoroethanol monitored by pulsed field gradient NMR diffusion measurements. *J. Biomol. NMR* 2000; **16**: 109–119.

22. Piotto M, Saudek V, Sklenar V. Gradient tailored excitation for single quantum NMR spectroscopy of aqueous solutions. *J. Biomol. NMR* 1992; **2**: 661–665.

23. Wishart DS, Bigam CG, Yao J, Abidgaard F, Dyson HJ, Oldfield E, Markley JL, Sykes BD. 1H, 13C and 15N chemical shift referencing in biomolecular NMR. *J. Biomol. NMR* 1995; **6**: 135–140.

24. Gibbs SJ, Johnson Jr CS. A PFG NMR experiment for accurate diffusion and flow studies in the presence of eddy currents. *J. Magn. Reson.* 1991; **93**: 395–402.

25. Dingley AJ, Mackay JP, Chapman BE, Morris MB, Kuchel PW, Hambly BD, King GF. Measuring protein self-association using pulsed field gradient NMR spectroscopy: Application to myosin light chain 2. *J. Biomol. NMR* 1995; **6**: 321–328.

26. Stejskal EO, Tanner JE. Spin diffusion measurements: spin echoes in the presence of a time-dependent field gradient. *J. Chem. Phys.* 1965; **42**: 288–292.

27. Skowronek M, Stopa B, Konieczny L, Rybarska J, Piekarska B, Szneler E, Bakalarski G, Roterman I. Self-assembly of Congo red — a theoretical and experimental approach to identify its supramolecular organization in water and salt solutions. *Biopolymers* 1998; **46**: 267–281.

28. Altieri AS, Hinton DP, Byrd RA. Association of biomolecular systems via pulsed field gradient NMR self-diffusion measurements. *J. Am. Chem. Soc.* 1995; **117**: 7566–7567.

29. Pan H, Barany G, Woodward C. Reduced BPTI is collapsed. A pulsed field gradient NMR study of unfolded and partially folded bovine pancreatic trypsin inhibitor. *Protein Sci.* 1997; **6**: 1985–1992.

30. Ilyina E, Roongta V, Pan H, Woodward C, Mayo KH. A pulsed-field gradient NMR study of bovine pancreatic trypsin inhibitor self-association. *Biochemistry* 1997; **36**: 3383–3388.

31. Teller DC, Swanson E, de Haen C. The translational friction coefficient of proteins. *Methods Enzymol.* 1979; **61**: 103–124.

32. Price WS, Tsuchiya F, Arata Y. Lysozyme aggregation and solution properties studied using PGSE NMR diffusion measurements. *J. Am. Chem. Soc.* 1999; **121**: 11 503–11 512.